International Journal of Thermophysics, Vol. 7, No. 4, 1986

Noble Gas–Carbon Dioxide Thermal Diffusion Factors: Anomalous Behavior for Ar/Co_2 [1]

W. L. Taylor[2,3] and P. T. Pickett[2]

Thermal diffusion factors for equimolar mixtures of neon and argon with carbon dioxide have been measured in the temperature range from 250 to 700 K. The data were obtained in a 20-tube trennschaukel, or "swing separator." The Ne/CO_2 system demonstrated the expected increase in α_T with increasing temperature as predicted by the Chapman–Enskog theory using spherically symmetrical interaction potentials and elastic collisions. The thermal diffusion factor for Ar/CO_2, however, demonstrated an inverse temperature effect which is not explained by the simplified kinetic-theory model used for the calculation. While this effect has ben observed by other workers, the present data exhibit a less precipitous decrease with temperature. Using interaction potentials available in the literature, it was possible to calculate theoretically accurate values of α_T for Ne/CO_2 but not for Ar/CO_2. In the latter case the small mass difference produced very small values of α_T, the peculiar behavior of which undoubtedly lies in nonnegligible asymmetric and inelastic effects not taken into account in the calculations.

KEY WORDS: argon; carbon dioxide; mixtures; neon; thermal diffusion factor.

1. INTRODUCTION

A controversy has existed for several decades over the anomalous behavior of the thermal diffusion factor, α_T, of noble gas/CO_2 mixtures. Studies of well over a hundred systems indicate that for by far the majority, α_T increases in magnitude with increasing temperature. Waldmann [1] first observed an anomalous effect for Ar/CO_2 some 35 years ago when he investigated the diffusion thermoeffect for 10 mixtures of gases containing

[1] Paper presented at the Ninth Symposium on Thermophysical Properties, June 24–27, 1985, Boulder, Colorado, U.S.A.

[2] Monsanto Research Corporation—Mound, Miamisburg, Ohio 45342, U.S.A.

[3] Department of Chemistry, University of Cincinnati, Cincinnati, Ohio 45221, U.S.A.

0195-928X/86/0700-0837$05.00/0

polyatomics. The Ar/CO_2 system was the only one in which α_T demonstrated a negative temperature effect. About a decade later Weissman et al. [2] reported a similar but smaller such effect for Ne/CO_2 from measurements made in a two-bulb apparatus. This group attempted to calculate theoretical values of α_T within the framework of the Chapman–Enskog theory but failed to find a satisfactory force model which yielded α_T. In the next two decades a handful of groups examined the $Ar–CO_2$ system and observed the negative temperature effect. Cozens and Grew [3] used a two-bulb method and obtained a decreasing α_T which exhibited a positive minimum around 500 K and increased at temperatures above this. Batabyal et al. [4] were the first to employ a trennschaukel, using a four-tube device in which they measured an extremely steep negative temperature effect between 300 and 400 K. A similar effect was observed by Shashkov et al. [5] around 325 K in a two-bulb apparatus. Trengove and Dunlop [6], who have developed a two-bulb apparatus capable of very great accuracy in a limited temperature range, investigated $Ne–CO_2$ between 270 and 324 K, discovering that α_T actually increases with temperature, in contrast to the results reported by Weissman et al. [2]. They also found that the $Ne–CO_2$ measurements of Batabyal and Barua [7], conducted in an eight-tube trennschaukel, were about 30% high. Trengove and Dunlop were unfortunately unable to make successful measurements on $Ar–CO_2$ and, indeed, it was Dunlop who suggested this project to the authors.

2. EXPERIMENTAL

2.1. Description of the Apparatus

A schematic diagram of the experimental apparatus is shown in Fig. 1. The device is designed basically to sustain a temperature difference of ΔT between two isothermal regions, one held at T_H (upper) and the other held at T_C (lower). The trennschaukel, or "swing separator," (A) consists of two solid nickel blocks in the shape of a cylinder with a hole in the middle. Twenty equally spaced 0.02-m-i.d. holes were bored 0.05 m deep in each block, then the two blocks were connected with 0.02–m–i.d. Inconel tubes approximately 0.05 m long which were heliarc welded into the blocks. Before assembly, a spiral of stainless-steel mesh mounted on a central post was screwed into the bottom of each hole to assist thermal equilibration of the gas to the block temperature. Inconel capillaries 0.0015-m-i.d. connect each of the approximately 0.15-m-long tubes thus formed top to bottom in the interior of the torus. Channels have been machined in the lower block which are connected at a number of points around the circumference to a

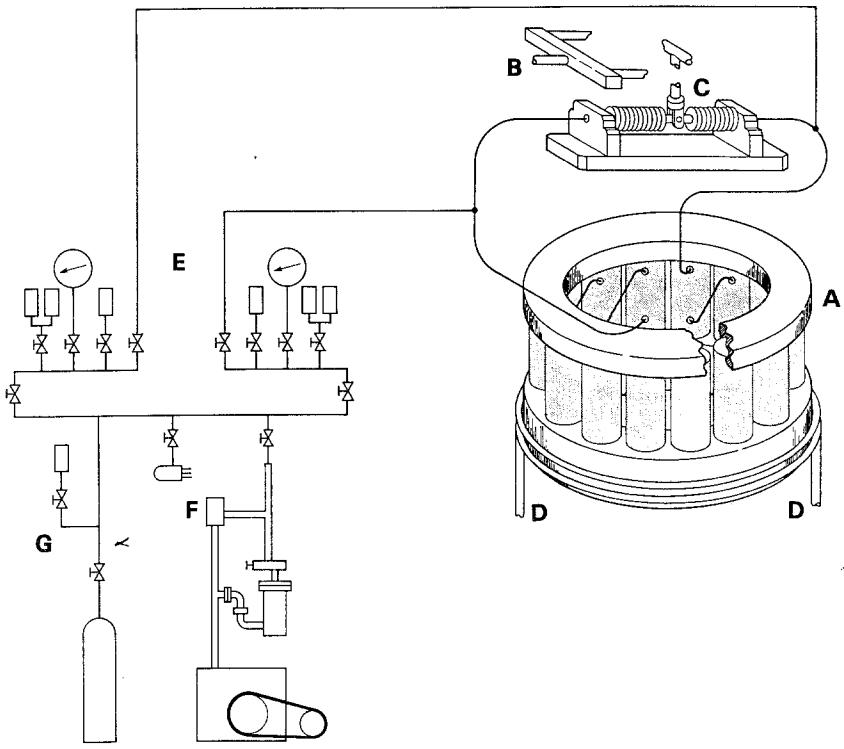

Fig. 1. Schematic of apparatus. A, 20-tube trennschaukel; B, drive shaft to pump mechanism; C, bellows pump; D, lower block cooling manifold; E, sampling ports; F, vacuum system; G, feed gas supply.

cooling manifold (D). Either room temperature compressed air or cold nitrogen gas boiled off from LN_2 dewars is circulated through the manifold to cool the lower block. Both the manifold and the lower block are encased in an insulating material. The bellows pump (C) is mounted directly above the upper block and is driven through the drive shaft (B) by a sinusoidal cam. The pump mechanism provides a variable preselected stroke (e.g., volume pumped) and pump rate. One bellows is connected by a capillary to the top of the first tube and the other bellows is connected to the bottom of the twentieth tube. The trennschaukel and bellows pump are mounted in an environmental chamber. The loading and sampling system (E) consists of a "hot" side and a "cold" side tied into the bellows capillaries mentioned above. There are three sample ports and a Wallace and Tiernan gauge on each side connected to a vacuum manifold wherein pressure is monitored by a thermocouple/ion gauge. The vacuum system (F), consisting of a dif-

fusion pump backed by a mechanical pump, and the feed gas cylinder with sample port (G) connect into the vacuum manifold.

The temperature control and monitoring system are based upon chromel–alumel thermocouples. A master thermocouple is embedded in the top block of the trennschaukel and this controls the selected temperature T_H by supplying power to the environmental chamber through a proportional-integral (reset)-derivative (rate), or PID controller. A reference thermocouple is also embedded in the top block near the master thermocouple. Twenty-four additional thermocouples are mounted in either wells or slots in the blocks and tubes as follows: six junctions are mounted in each of four equally spaced (90°) locations around the device. In each quadrant containing six junctions, two are mounted in the top block, two on the connecting tube, and two in the bottom block. All of the thermocouples are wired to read the Δemf's versus the reference thermocouple. Finally, a master thermocouple pair with one junction embedded in the top block and the other in the bottom block controls the preselected ΔT for the experiment by calling for more or less cooling gas to the manifold through a second PID controller. The actual temperatures in the hot and cold blocks are then obtained by reading the eight Δemf's of the thermocouple pairs from each of the upper and lower blocks with a digital voltmeter to $\pm 1\ \mu$V.

2.2. Operation of the Apparatus

Conducting an accurate experiment in a trennschaukel is subject to some restrictions in the selection of operating parameters. The basic premise in using a trennschaukel instead of a single stage, or "two-bulb" device is to cascade the separation (which is inherently small) so that a comparatively more accurate analysis can be made of the separation obtained. The relatively slow to-and-fro pumping of the gas superimposed upon the relatively fast thermal diffusion transports the light species to the hot and the heavy species to the cold end of the device. The separation is increased over a single stage n-fold, where n is the number of tube/capillary pairs.

Van der Waerden [8] has provided a theoretical treatment of gas transport in a trennschaukel which expresses the approach to the steady state as a set of $n+2$ time-dependent differential equations as a function of the composition. Resulting from this study are several factors which must be considered when operating the device. Simultaneous treatment of these four factors was accomplished by computer simulation of an experiment with various operating conditions with a view to minimizing the unwanted effects. To be considered are (i) the compression of gas in the middle

stages, (ii) the approach to the steady state, (iii) back diffusion in the capillaries, and (iv) enhanced enrichment due to pumping. The first of these factors arises as a result of frictional flow resistance (Poiseuille's Law) in the capillaries, which decreases the volumetric flow from stage to stage, reaching a minimum in the middle tubes. A range of pump rate and pumped volume was determined so that the compression in the middle tubes did not exceed approximately 6% as suggested by Van der Waerden. The other three factors appear as corrections to the measured compositions obtained at the end of the experiment and cannot be eliminated entirely. Explicit expressions for these three corrections as derived by Van der Waerden and the way in which they are used to correct the observed composition difference in the experiments are given elsewhere [9]. Application of corrections (ii) and (iii) slightly increases the observed composition difference, while (iv) decreases it. Because of this offsetting effect, it was possible with the computer simulation nearly to balance the correction factors in addition to minimizing them individually. By this means, the individual corrections were kept to not larger than approximately 3.5% and were balanced to 1% or better so that the details need not be repeated here.

The selected conditions for the experiments were in the following ranges: temperature, 250 to 700 K; pressure, 1280 to 7500 $N \cdot m^{-2}$; pump rate, 70 to 100 s/cycle; and pumped volume, 2 to 4×10^{-6} m^3/(half stroke). The ΔT's used were selected to be approximately 15% of the absolute average temperature for Ne–CO_2 and approximately 25% for Ar–CO_2. With the desired temperatures stabilized, an equimolar gas mixture of either Ne– or Ar–CO_2 was loaded to the desired pressure and a feed gas sample was taken. The experiments were run for a minimum of five half-lives so that compositions were closer than 0.5% to the theoretical steady-state value. Thus an experiment was conducted over a period of 1 to 2 days, depending upon the temperature. At the end of the experiment the capillaries leading into the trennschaukel were purged by drawing a small volume simultaneously from the hot and cold side into the single sample ports. Immediately thereafter, duplicate samples were simultaneously drawn into the dual sample ports. The feed plus hot and cold side duplicate samples were analyzed on a highly modified microprocessor-controlled CEC 620A mass spectrometer. This machine was calibrated before and after each set of samples was run by volumetric standards, approximately equimolar, which were prepared with an accuracy of 0.1% [10].

The gases used for both the calibration standards and the experiments were as follows: argon, 99.996% pure; carbon dioxide, 99.99% pure; and neon-20, 99.97% mass 20 in total neon prepared in Mound's thermal diffusion columns from natural isotopic abundance neon of 99.94% purity.

3. RESULTS

3.1. Experimental Results

The present measurements were carried out in the temperature range of 250 to 700 K at intervals of 75 K. Two experiments were conducted at each temperature in order to ensure reproducibility. The Ne–CO_2 results are given in Table I, and the Ar–CO_2 data are listed in Table II. The second column in the table represents the "average" temperature assigned to the measurement of α_T and is the geometric mean of T_H and T_C. The experimental thermal diffusion factor was calculated from the fundamental relation

$$\alpha_T = \ln q / \ln(T_H/T_C) \tag{1}$$

where q is the separation factor for a single stage defined as the ratio of compositions at T_H to the ratio at T_C. The three correction factors cited in

Table I. Temperature Dependence of the Thermal Diffusion Factor for an Equimolar Mixture of ^{20}Ne–CO_2

$T=(T_1T_2)^{1/2}$ (K)	α_T	Correction[a]			Uncertainty[b]			
		A	B	C	D	E	F	G
250	0.136	0.977	1.034	0.975	1.8	1.3	3.1	1.9
250	0.132	0.985	1.034	0.975	0.6	1.6	2.2	
325	0.157	0.986	1.035	0.973	0.4	3.2	3.6	3.0
325	0.159	0.986	1.035	0.973	1.8	3.1	4.9	
401	0.175	0.995	1.035	0.973	6.4	5.3	11.7	7.3
403	0.164	0.986	1.035	0.973	1.3	10.9	12.2	
403	0.167	0.992	1.035	0.973	3.4	10.6	14.0	
473	0.177	0.997	1.031	0.970	1.9	11.0	12.9	9.2
473	0.173	0.996	1.032	0.970	2.0	11.1	13.1	
551	0.185	0.999	1.030	0.967	0.6	9.4	10.0	8.1
551	0.179	0.985	1.031	0.968	3.4	9.6	13.0	
626	0.189	0.994	1.031	0.969	5.4	10.7	16.1	10.4
627	0.188	0.999	1.035	0.972	2.6	10.6	13.2	
702	0.184	0.995	1.030	0.967	2.2	12.2	14.4	10.4
702	0.185	0.997	1.030	0.967	3.7	11.4	15.1	

[a] (A) Correction due to the exponential approach to steady state; (B) correction due to the disturbance due to pumping; (C) correction due to back difusion in the capillaries.

[b] (D) Uncertainty due to composition analysis; (E) uncertainty due to temperature measurements; (F) total uncertainty; (G) average total uncertainty divided by $\sqrt{n}$, where n is the number of duplicate experiments.

Table II. Temperature Dependence of the Thermal Diffusion Factor for an Equimolar Mixture of Ar–CO_2

$T=(T_1T_2)^{1/2}$ (K)	α_T	Correction[a] A	B	C	Uncertainty[b] D	E	F	G
247	0.0213	0.969	1.033	0.973	2.7	1.6	4.2	3.0
247	0.0204	0.974	1.034	0.974	3.0	1.4	4.4	
324	0.0183	0.977	1.037	0.977	11.6	2.4	14.0	11.8
324	0.0171	0.978	1.037	0.977	16.6	2.7	19.3	
401	0.0151	0.950	1.030	0.968	16.6	2.3	18.9	7.4
401	0.0141	0.985	1.030	0.968	2.8	2.1	4.9	
401	0.0133	0.985	1.030	0.968	12.5	2.1	14.6	
475	0.0135	0.994	1.030	0.968	12.7	6.4	19.1	10.7
475	0.0123	0.989	1.031	0.969	4.8	6.3	11.1	
550	0.0110	0.983	1.031	0.970	20.7	7.2	27.9	18.5
550	0.0100	0.990	1.031	0.969	11.1	7.4	18.5	
550	0.0092	0.988	1.031	0.969	42.3	7.4	49.7	
624	0.0096	0.992	1.030	0.968	7.3	8.0	15.3	14.2
624	0.0094	0.990	1.030	0.968	17.0	8.0	25.0	
703	0.0068	0.997	1.031	0.967	16.5	9.1	25.6	16.0
703	0.0061	0.996	1.031	0.968	10.5	9.2	19.7	

[a] (A) Correction due to the exponential approach to steady state; (B) correction due to the disturbance due to pumping; (C) correction due to back difusion in the capillaries.

[b] (D) Uncertainty due to composition analysis; (E) uncertainty due to temperature measurements; (F) total uncertainty; (G) average total uncertainty divided by $\sqrt{n}$, where n is the number of duplicate experiments.

the previous section (2.2) are applied to the composition differences attained in the experiment between the average of the hot and cold side duplicate samples by dividing this difference for each component by the product of the corrections A, B, and C from the tables. Rearranging the separation factor in terms of the corrected composition differences, $\Delta\chi$, one has

$$\ln q = \frac{1}{n}\frac{1+(\Delta\chi/\chi_1)}{1+(\Delta\chi/\chi_2)} \tag{2}$$

where the subscript 1 refers to the light species and 2 refers to the heavy species. The convention is that q is positive if the heavy component concentrates at the cold end. Here χ_1 and χ_2 are as measured at T_C and n is the number of stages.

The denominator of Eq. (1) must also be rearranged in order to make use of the multiple thermocouples described in Section 2.1 which track the hot and cold block temperatures, thus providing accurate averages for the experiment. Therefore,

$$\ln(T_H/T_C) = \frac{1}{k}\sum_{i=1}^{k} \ln\left(1 + \frac{\Delta T_i}{T_C}\right) \tag{3}$$

where k in this case is eight and represents the thermocouple pairs in the top and bottom blocks. The uncertainties listed in columns D and E were obtained from the partial differentials of Eq. (1). The difference in the mass spectrometer analyses for the duplicate samples was used to obtain the estimated uncertainty in composition. The observed temperature fluctuation and/or drift was used to estimate the uncertainty in temperature. Column F represents the total estimated uncertainty for a given experiment.

The present results, calculated from Eq. (1) and represented by the filled circles, are shown for Ne–CO_2 in Fig. 2 and Ar–Co_2 in Fig. 3. The error bars represent the overall estimated experimental uncertainty at a given temperature from column G in the tables.

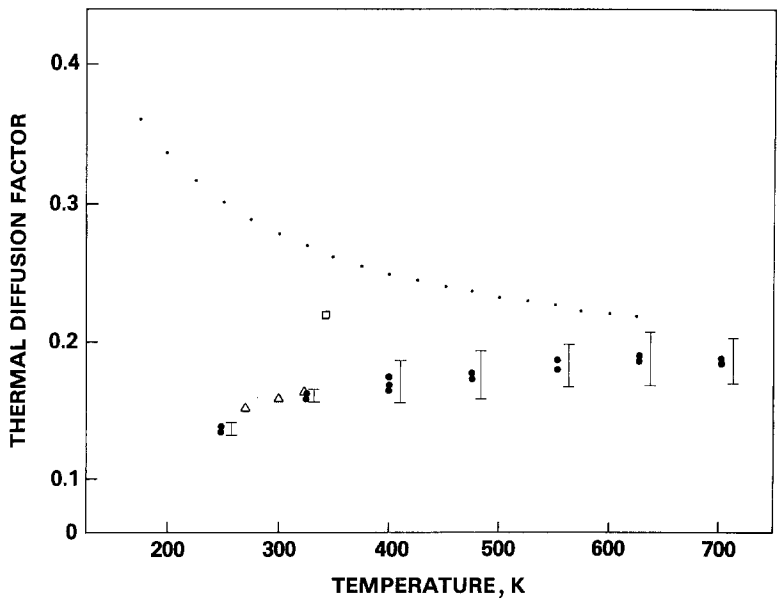

Fig. 2. Thermal diffusion factor for ^{20}Ne–CO_2. The experimental points are (●) present data, (△) Trengove and Dunlop (6), (□) Batabyal and Barua (7), and (···) smoothed data of Weissman et al. (2).

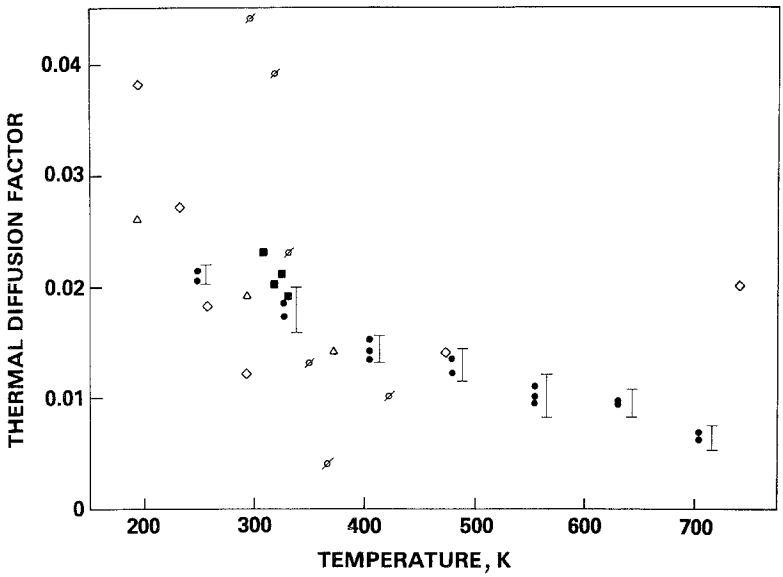

Fig. 3. Thermal diffusion factor for Ar–Co_2. The experimental points are (●) present data, (△) Waldmann (1), (◇) Cozens and Grew (3), (∅)Batabyal et al. (4), and (■) Shashkov et al. (5).

3.2. Least-Squares Analysis of Results

In order to define better the temperature dependence of the two systems, the present data were subjected to a least-squares analysis. Previous work [11–13] has indicated that a suitable empirical function could be constructed from some combination of powers of $T^{1/2}$. We used 92 trial functions consisting of a constant plus all combinations of one to three additional terms from the general polynomial

$$\alpha_T = \sum_n C_n T^{n/2}; \qquad n = 0,..., \pm 4 \tag{4}$$

for fitting the data. We sought to minimize the average rms percentage deviation of the experimental points from the function. Some interesting results were obtained. In neither case did a four-term function give the lowest rms percentage deviation. In fact for Ne–CO_2 a two-term function was best. The best choice for a function which represented both systems was $\alpha_T = C_0 + C_1/T + C_2 T^2$. The explicit expressions are

$$\alpha_T = 0.23085 - 23.779/T - 0.20576 \times 10^{-7} T^2 \tag{5}$$

for $Ne–CO_2$ (rms deviation = 1.9 %) and

$$\alpha_T = 0.84684 \times 10^{-2} + 3.2805/T - 0.12918 \times 10^{-7} T^2 \quad (6)$$

for $Ar–CO_2$ (rms deviation = 7.3 %). The functional form $\alpha_T = C_0 + C_1/T^{1/2} + C_2/T$ which was used in Ref. 11 was also very good.

3.3. Theoretical Results and Discussion

The third-order Chapman–Enskog approximation, $[\alpha_T]_3$, was calculated by means of Eq. (1) in Ref. 9 using published intermolecular potentials [14–19] for the pure species and the usual combining rules for

Table III. Potentials and Force Parameters Used for the Theoretical Calculations

Interaction	Potential	ε/k (K)	σ (Å)	r_m (Å)	Ref. No.
	(A) Potentials given in the literature				
Ne–Ne	Lennard-Jones, 12-6 (LJ1)	35.7	2.789	—	14
	Hartree–Fock dispersion (HFD1)	42.25	—	3.087	15
Ar–Ar	Lennard–Jones, 12-6 (LJ2)	124.0	3.418	—	14
	Hartree–Fock dispersion (HFD2)	143.2	—	3.759	16
CO_2–CO_2	Lennard–Jones, 12-6 (LJ3)	190.0	3.996	—	14
	Atom to atom, Exp-6 (RUS)	172.01	—	5.830	17
	Lennard–Jones, 12-6 (LJ4)	537.0	3.05	—	18
$Ar–CO_2$	Parker–Snow–Pack (PSP) (spherically symmetric interaction)	98.0	—	4.342	19
	(B) Potentials for the unlike interactions formed from the combining rules $\sigma_{12} = (\sigma_1 + \sigma_2)/2$ and $\varepsilon_{12} = (\varepsilon_1 \varepsilon_2)^{1/2}$				
$Ne–CO_2$	Lennard–Jones, 12-6 (LJ5) (combining LJ1 and LJ3)	82.36	3.392	—	—
	Lennard–Jones, 12-6 (LJ6) (combining HFD1 and LJ4)	150.6	2.904	—	—
	Lennard–Jones, 12-6 (LJ7) (combining HFD1 and RUS)	85.25	4.002	—	—
$Ar–CO_2$	Lennard–Jones, 12-6 (LJ9) (combining LJ2 and LJ3)	153.0	3.707	—	—
	Lennard–Jones, 12-2 (LJ10) (combining HFD2 and LJ4)	277.3	3.200	—	—

the mixtures. Monatomic gas theory, which usually yields a fair representation of thermal diffusion, was employed for the calculations because a treatment of nonspherical interactions was beyond the scope of this work. As pointed out, however, by Monchick et al. [20], when the mass/size effect (normally dominant in an interaction) is very small, a second term in α_T due to inelastic collisions may become nonnegligible. That apparently is the case for Ar–Co_2 but not for Ne–CO_2, as will be shown.

The potentials used varied considerably in complexity and parameters and details may be found in the references. The transport collision integrals which appear in the matrix elements of $[\alpha_T]_3$ are a function of the intermolecular potential and were calculated for the like and unlike interaction by the method of Keller and Taylor [21]. The various published potentials investigated, along with the constructed potentials for the mixtures, are given in Table III.

Ne–CO_2 exhibits a normal temperature dependence which is verified in both trend and magnitude by the highly accurate measurements of Trengove and Dunlop [6]. We found one combination of potentials which did a reasonable job of representing α_T for this system. This combination consisted of the accurate HFD1 [15] for neon and a deep-well [18] Lennard–Jones potential for CO_2/CO_2. Using the combining rules for

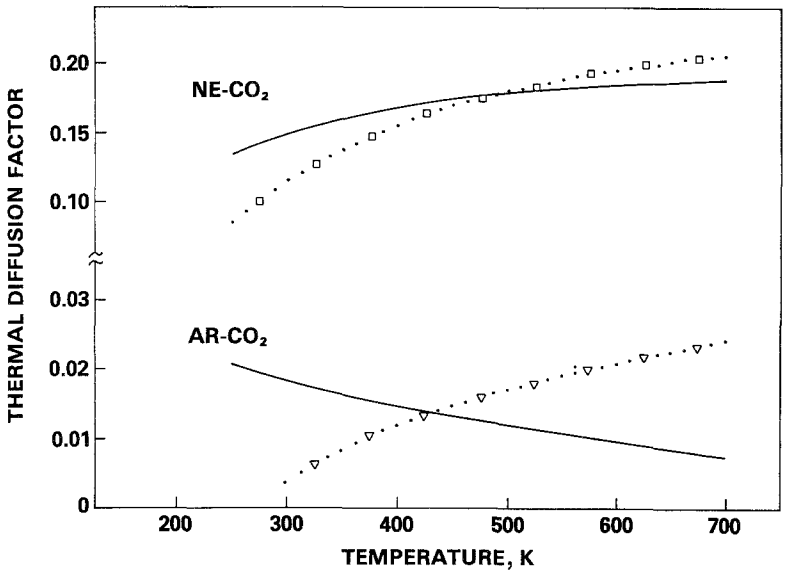

Fig. 4. Comparison of theoretical thermal diffusion factor, $[\alpha_T]_3$, to least-squares fit of present data. The upper curves are (——) Eq. (5) and (· □ ·) HFD1/LJ4/LJ6. The lower curves are (——) Eq. (6) and (· ▽ ·) HFD2/LJ4/LJ10.

Ne–CO_2, we obtained a curve of approximately the correct magnitude but which drops off somewhat too rapidly at lower temperatures as shown in Fig. 4.

Published potentials for Ar and Ar–CO_2 were examined in a similar fashion but none were found which predicted an inverse temperature effect. The HFD2 [16] potential for argon along with the same CO_2 potential [18] found most suitable for the Ne–CO_2 calculation was the only combination which came anywhere near yielding the proper magnitude for α_T for Ar–CO_2. These calculations did not, however, yield the proper temperature dependence as can be seen in the lower half of Fig. 4. The failure to find a satisfactory potential for Ar–CO_2 probably lies in the fact that nonspherical and inelastic effects were neglected in the kinetic-theory formulation used for the calculations. This is not entirely surprising in that Kestin et al. [22] observed anomalous behavior in the thermal conductivity of Ar–CO_2 which also could not be represented even quantitatively by existing kinetic-theory expressions. We therefore conclude that the second term in α_T which is sensitive to inelastic collisions [20] must be included for Ar–CO_2, if not for Ne–CO_2, and that future theoretical work should be directed at evaluating this inelastic contribution to thermal diffusion.

ACKNOWLEDGMENT

Mound is operated by Monsanto Research Corporation for the U.S. Department of Energy under Contract DE-AC04-76-DP00053.

REFERENCES

1. L. Waldmann, *Z. Naturforsch.* **4a**:105 (1949).
2. S. Weissman, S. C. Saxena, and E. A. Mason, *Phys. Fluids* **4**:643 (1961).
3. J. R. Cozens and K. E. Grew, *Phys. Fluids* **7**:1395 (1964).
4. A. K. Batabyal, A. K. Ghosh, and A. K. Barua, *J. Chem. Phys.* **48**:5238 (1968).
5. A. G. Shashkov, A. F. Zolotukhina, T. N. Abramenko, B. P. Mathur, and S. C. Saxena, *J. Phys. B Mol. Phys.* **12**:3619 (1979).
6. R. D. Trengove and P. J. Dunlop, *Chem. Phys. Lett.* **94**:118 (1983).
7. A. K. Batabyal and A. K. Barua, *J. Chem. Phys.* **48**:2557 (1968).
8. B. L. Van der Waerden, *Z. Naturforsch.* **12a**:583 (1957).
9. W. L. Taylor, S. Weissman, W. J. Haubach, and P. T. Pickett, *J. Chem. Phys.* **50**:4886 (1969).
10. (a) R. E. Ellefson, R. W. Baker, and J. T. Gill, MLM-2574 NTIA (Nov. 1978); (b) R. W. Baker, T. L. Buxton, and R. E. Ellefson, *Rev. Sci. Instrum.* **50**:1429 (1979).
11. K. E. Grew and T. L. Ibbs, *Thermal Diffusion in Gases* (Cambridge University Press, Cambridge, England, 1952).
12. S. Weissman, *Phys. Fluids* **12**:2237 (1969).

13. W. L. Taylor, *J. Chem . Phys.* **72**:4973 (1980).
14. J. O. Hirschfelder, C. F. Curtiss, and R. B. Bird, *Molecular Theory of Gases and Liquids* (John Wiley & Sons, New York, 1954).
15. R. A. Aziz, W. J. Meath, and A. R. Alnatt, *Chem . Phys.* **78**:295 (1983).
16. R. A. Aziz and C. H. Chen, *J. Chem. Phys.* **67**:5719 (1977).
17. L. I. Kitaigorodski, K. V. Mirskaga, and V. V. Nauchitel, *Sov. Phys. Crystallogr.* **14**:769 (1970).
18. T. B. MacRury and W. A. Steele, *J. Chem. Phys.* **64**:1288 (1976).
19. G. A. Parker, R. L. Snow, and R. T. Pack, *J. Chem. Phys.* **64**:1668 (1976).
20. L. Monchick, S. I. Sandler, and E. A. Mason, *J. Chem. Phys.* **49**:1178 (1968).
21. (a) J. M. Keller and W. L. Taylor, *J. Chem. Phys.* **51**:4829 (1969); (b) W. L. Taylor, Report MLM-2661, UC-34a, Monsanto Res. Corp., Miamisburg, Ohio (1979).
22. J. Kestin, Y. Nagasaka, and W. A. Wakeham, *Physica* **113A**:1 (1982).